Dipole-Pomeron model in proton-proton inclusive and exclusive processes

N. G. Antoniou, C. B. Kouris, and G. M. Papaioannou
Nuclear Research Center "Demokritos," Aghia Paraskevi Attikis, Greece

E. K. Manesis
Physics Department, University of Ioannina, Greece

(Received 9 April 1975)

A model with a simple pole and a double pole for the inclusive Pomeranchuk singularity has been considered. The factorization of this singularity together with the weak-coupling approximation leads to a two-component mechanism for the production processes. Self-consistency of the dipole Pomeron leads to intercept one for this singularity and a meson trajectory is generated in the exclusive process. Phenomenological implications of the model concerning multiplicity distributions and rapidity two-particle exclusive distributions are examined and a comparison with data is made.

I. INTRODUCTION

From the study of the hadronic phenomena at high energies it has been established that the multiperipheral model constitutes a zero-order approximation to the hadronic world, at least for the energy region covered by Fermilab and the CERN ISR. The hierarchy of the dynamical mechanisms which play a role in the production phenomena can be easily generated in terms of Regge singularities, by a systematic study of the Mueller diagrams in the asymptotic region of rapidity differences of the inclusively produced particles. In fact, the exchange of a simple, factorizable Regge pole with intercept $\alpha(0) \cong 1$ (Pomeron) in the diagrams of Fig. 1 leads to the Chew-Pignotti model for the production amplitude.[1] It corresponds to a Poisson distribution for the partial inelastic cross sections, which means that the particles are produced uncorrelated. On the other hand, the phenomenon of rising cross sections suggests that the Pomeranchuck singularity has a hard component (more singular than a simple pole) which may be a double or triple pole at $j = 1$ leading to a $\ln s$ or $\ln^2 s$ behavior of the total cross section. In general, the hard component of the Pomeranchuck singularity may be a branch point at $j = 1$ leading to a $(\ln s)^{\epsilon}$ behavior of the total cross section $(1 < \epsilon < 2)$. This last behavior is suggested by the models of a renormalized Pomeron within the Gribov's Reggeon calculus.[2] This new component of the Pomeranchuck singularity is expected to play a role in the production mechanism when it is exchanged in the Mueller diagrams of Fig. 1. In fact a hard singularity is expected to be factorizable by a naive generalization of the properties of Regge singularities in the two-body amplitudes. Hence, the effect of such a Regge-Mueller singularity on the production phenomena could be easily studied owing to factorization. However, we have shown in a previous work[3] that in order that the factorization of a hard singularity at $j = 1$ in the Mueller diagrams be not in conflict with positivity the self-coupling of such a component in these diagrams has to be zero. With this condition one can easily formulate the problem of hadronic production at high energies using the Bardeen-Peccei formalism which relies upon the factorization in the Mueller diagrams.[4] In this paper we take as a good candidate for the hard component of the Pomeranchuck singularity a double pole at $j = \alpha_P(0)$. This model is supported by the phenomenological study of the ISR data on pp elastic scattering which reveals the remarkable property of geometrical scaling.[5] In fact, from geometrical scaling $\sigma_t \sim R^2(s)$ plus logarithmic shrinking due to a moving singularity $(R \sim \ln s^{1/2})$, we obtain the dipole behavior, $\sigma_t \sim \ln s$.

In the physically interesting approximation of a weak coupling between the simple and the double pole in the Mueller diagrams (Fig. 1) we find that the hard component of the Mueller-Pomeranchuck singularity (dipole Pomeron) generates a diffractive component in the production mechanism. Hence, we arrive at the conclusion that the two components of the Pomeranchuck singularity (simple and double poles) in the Mueller diagrams correspond to the well-known components of the pro-

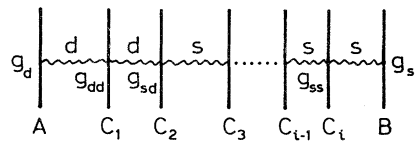

FIG. 1. The Mueller-Regge diagram for the inclusive production of i particles with simple and double Pomeron exchanges.

duction mechanism, the multiperipheral (short-range) component and the diffractive component which produces long-range correlations.

II. THE MODEL

We consider the inclusive process $A+B \to C_1C_2\cdots C_iX$ where the initial hadrons (protons) A and B produce inclusively i identical particles (pions) with large rapidity differences. Following Ref. 4 we write the generating function:

$$I(z, Y)=\sum_{n=0}^{\infty}\sigma_n(Y)(1+z)^n \ , \tag{1}$$

where $\sigma_n(Y)$ is the partial cross section for the production of n particles and $Y=Y_b-Y_a$ is the rapidity difference of the initial hadrons A and B.

From the definition (1) we obtain

$$I(z=0)=\sigma_{\text{tot}} \ , \quad \left(\frac{\partial^i I(z, Y)}{\partial z^i}\right)_{z=0}=\rho_i(Y) \ , \tag{2}$$

where

$$\rho_i(Y)\equiv\langle n(n-1)\cdots(n-i+1)\rangle\,\sigma_{\text{tot}} \ . \tag{3}$$

In terms of the inclusive distributions

$$\rho_i(Y)=\int\frac{d^3p_1}{E_1}\cdots\frac{d^3p_i}{E_i}\left(\frac{E_1\cdots E_i\,d\sigma_{\text{in}}}{d^3p_1\cdots d^3p_i}\right) \ . \tag{4}$$

Taking the derivatives of $I(z, Y)$ at $z=-1$ we have

$$I(z=-1, Y)=\sigma_{\text{el}}(Y) \ , \tag{5}$$

$$\frac{1}{n!}\left(\frac{\partial^n I(z, Y)}{\partial z^n}\right)_{z=-1}=\sigma_n(Y) \ . \tag{6}$$

The knowledge of the generating function $I(z, Y)$ leads through Eqs. (5) and (6) to the determination of the multiplicity distribution $\sigma_n(Y)$.

The basic assumption in our model is that the inclusive distribution is dominated by the Regge-Mueller diagrams of Fig. 1, where the two components of the Pomeranchuk singularity (simple pole and double pole) are exchanged and the self-coupling of the double pole is zero, $g_{dd}=0$.[6] Then Eq. (4) is written as follows:

$$\rho_i(Y)=e^{-Y}i!\int_0^Y dz_1\int_0^{Y-z_1}dz_2\cdots\int_0^{Y-\sum_{\mu=1}^{i-1}z_\mu}dz_i\,g^+S(z_1)\,GS(z_2)\cdots S\left(Y-\sum_{\mu=1}^{i}z_\mu\right)g \ , \tag{7}$$

where g^+ is the row matrix of the external couplings of the exchanged factorizable singularities, G is the square matrix of the internal couplings, and $S(z)$ is the square matrix of the propagators of these singularities at $j=\alpha_P(0)$.[4] In our model, these matrices are

$$G=\begin{pmatrix} g_{ss} & g_{sd} \\ g_{sd} & 0 \end{pmatrix} \ ,$$

$$S(z)=\begin{pmatrix} 1 & 0 \\ 0 & z \end{pmatrix} e^{z\alpha_P(0)} \ , \tag{8}$$

$$g^+=(g_s, g_d) \ .$$

Then the generating function $I(z, Y)$ satisfies the following integral equation[4]:

$$\tilde{I}(z, Y)=\tilde{\rho}_0(Y)+z\int_0^Y dy\,\tilde{\rho}_0(y)\,G\tilde{I}(z, Y-y) \ , \tag{9}$$

where

$$\begin{aligned} &I(z, Y)=g^+\tilde{I}(z, Y)\,g, \\ &\rho_i(Y)=g^+\tilde{\rho}_i(Y)\,g \ , \\ &\tilde{\rho}_0(Y)=e^{-Y}S(Y) \ . \end{aligned} \tag{10}$$

The solution of (9) is

$$I(z, Y)=\frac{1}{2\pi i}\int_{c-i\infty}^{c+i\infty}d\theta\,e^{\theta Y}g^+\frac{1}{\tilde{\rho}_0^{-1}(\theta)-zG}\,g \ , \tag{11}$$

where $\tilde{\rho}_0(\theta)$ is the Laplace transform of the matrix $\tilde{\rho}_0(Y)$. Using the matrices (8) of our model we find

$$g^+\frac{1}{\tilde{\rho}_0^{-1}(\theta)-zG}\,g=\frac{g_s^2(\theta+1-\alpha_P)^2+2g_sg_dg_{sd}z+g_d^2(\theta+1-\alpha_P-zg_{ss})}{(\theta+1-\alpha_P-zg_{ss})(1+\theta-\alpha_P)^2-z^2g_{sd}^2} \tag{12}$$

It is expected that the coupling g_{sd} is small since it is responsible for the scaling-breaking effect in the one-particle inclusive distribution. In fact the rising of the plateau due to the dipole exchange in this model is given by a term proportional to $g_{sd}\ln s$. Hence, the weak-coupling g_{sd} approximation is justified since the scaling-breaking effect is a small perturbation to the basic phenomenon observed at the ISR. There-

fore, keeping only linear terms in g_{sd}, we obtain from (11) and (12)

$$I(z, Y) = e^{Y(\alpha_P - 1)}\left[g_s^2 e^{z g_{ss} Y} + g_d^2 Y - \frac{2 g_s g_d g_{sd}}{g_{ss}}\left(Y - \frac{e^{z g_{ss} Y} - 1}{z g_{ss}}\right)\right] + O(g_{sd}^2) . \quad (13)$$

In this approximation (small g_{sd}) the elastic cross section is given by the following equation[6]:

$$\sigma_{el}(Y) = I(z = -1) = \left(g_d^2 - \frac{2 g_s g_d g_{sd}}{g_{ss}}\right) Y e^{Y(\alpha_P - 1)} + \frac{2 g_s g_d g_{sd}}{g_{ss}^2} e^{Y(\alpha_P - 1)} + \left(g_s^2 - \frac{2 g_s g_d g_{sd}}{g_{ss}^2}\right) e^{Y(\alpha_P - 1 - g_{ss})} . \quad (14)$$

The total cross section is correspondingly

$$\sigma_t(Y) = I(z = 0) = g_s^2 + g_d^2 Y . \quad (15)$$

The dynamical origin of the three terms in Eq. (14) can be easily recognized by the fact that the elastic cross section receives contributions from the two components of the Pomeranchuck singularity and from the exchange of a typical meson trajectory. In fact the first two terms of (14) are identified with the two components of the Pomeron (simple pole and double pole) whereas the third one is due to the exchange of a meson trajectory α_M. Moreover, it is plausible to assume that there is no interference between the meson and the Pomeron since in our model the meson contribution is real at $t = 0$ whereas the Pomeron is predominantly imaginary in the high energy domain. This means that the third term in Eq. (14) is a pure meson contribution and therefore one obtains the following self-consistency relations, ignoring logarithms in the meson exchange:

$$\alpha_P(0) - 1 = 2\alpha_P(0) - 2 \text{ and } \alpha_P(0) - 1 - g_{ss} = 2\alpha_M(0) - 2 . \quad (16)$$

From (16) we obtain

$$\alpha_P(0) = 1 \text{ and } \alpha_M(0) = 1 - \tfrac{1}{2} g_{ss} . \quad (17)$$

This result shows that the two-component inclusive Pomeron generates in a self-consistent way the exclusive Pomeron with $\alpha_P(0) = 1$. It also leads to an exclusive meson trajectory with $\alpha_M(0) = 1 - \frac{1}{2} g_{ss}$. These remarks lead to a plausible value for the coupling $g_{ss} \simeq 1$,[7] whereas the external couplings g_s and g_d may be fixed from the total cross section which rises at the ISR consistently with Eq. (15) and gives for the couplings $g_s \simeq 5.3$ mb$^{1/2}$ and $g_d \simeq 1.4$ mb$^{1/2}$. Therefore we are left with only one parameter, g_{sd}, which gives the fine structure of the generating function (13) and the deviation of $\sigma_n(Y)$ from the Poisson distribution. In fact, for the inelastic cross sections $\sigma_n(Y)$ $(n > 0)$ we obtain from Eqs. (6) and (13)

$$\sigma_n(Y) = g_s^2 e^{-g_{ss} Y} \frac{(g_{ss} Y)^n}{n!} + \frac{2 g_s g_d g_{sd}}{g_{ss}^2}\left[1 - e^{-g_{ss} Y} \sum_{k=0}^{k=n} \frac{(g_{ss} Y)^k}{k!}\right] . \quad (18)$$

On the other hand, the total inelastic cross section is given by the following equation:

$$\sigma_{in}(Y) = \sigma_{tot}(Y) - \sigma_{el}(Y) = \frac{2 g_s g_d g_{sd}}{g_{ss}} Y + \left(g_s^2 - \frac{2 g_s g_d g_{sd}}{g_{ss}^2}\right) + \left(\frac{2 g_s g_d g_{sd}}{g_{ss}^2} - g_s^2\right) e^{-g_{ss} Y} . \quad (19)$$

From Eq. (18) it follows that the coupling g_{sd}, namely the contribution of the inclusive dipole, generates a diffractive component in the cross section $\sigma_n(Y)$ which is a correction to the basic component coming from the exchange of the inclusive simple pole and corresponding to a Poisson distribution. The diffractive nature of the second component of $\sigma_n(Y)$ in Eq. (18) can be easily recognized from the fact that for fixed n and $Y \to \infty$, its contribution to $\sigma_n(Y)$ has a constant nonzero value $\sigma_n(\infty) = 2 g_s g_d g_{sd}/g_{ss}^2$, whereas the nondiffractive component goes to zero faster than any power of Y. With this interpretation of the two components in Eq. (18) we may write for the diffractive and nondiffractive parts of $\sigma_n(Y)$ the following equations:

$$\sigma_n^D(Y) = \frac{2 g_s g_d g_{sd}}{g_{ss}^2}\left[1 - e^{-g_{ss} Y} \sum_{k=0}^{k=n} \frac{(g_{ss} Y)^k}{k!}\right] , \quad (20)$$

$$\sigma_n^{ND}(Y) = g_s^2 e^{-g_{ss} Y} \frac{(g_{ss} Y)^n}{n!} . \quad (21)$$

For the total inelastic cross section we have correspondingly

$$\sigma_{in}^{ND}(Y) = g_s^2 (1 - e^{-g_{ss} Y}) , \quad (22)$$

$$\sigma_{in}^D(Y) = \frac{2 g_s g_d g_{sd}}{g_{ss}}\left[Y - \frac{1}{g_{ss}}(1 - e^{-g_{ss} Y})\right] . \quad (23)$$

From the last two equations it follows that the rising of the inelastic cross section is entirely due to the diffractive component, whereas the nondiffractive component goes to a constant value for $Y \to \infty$ and it saturates the constant background of the total cross section g_s^2. The logarithmic rise of $\sigma_{in}^D(Y)$ is consistent with a nonzero value of the triple Pomeron coupling $G_{sss}(0)$ provided that in the diffractive excitation process and in the Pomeron-proton cross section the only component of the

Pomeron which contributes is the simple pole. The dipole cannot excite diffractively the initial hadrons since this would lead to the usual disease $\sigma_{in}^{D} > \sigma_t$. For the same reason the dipole cannot contribute to the Pomeron-proton total cross section for both components of the Pomeron (simple and double). Moreover, the simple pole must be fixed since a moving simple pole would lead to the asymptotic behavior $\sigma_{in}^{D}(Y) \sim \ln Y$ in contrast to Eq. (23).

We observe that the smallness of the coupling g_{sd} may guarantee the smallness of the diffractive component even at high energies. In fact, from Eq. (23) we find that for a typical ISR energy, $Y = 7.5$, the diffractive cross section is 25% of the total inelastic cross section for $g_{sd} \simeq 0.1$.

On the other hand, the rise of the inelastic cross section, $\Delta\sigma_{in} = (2 g_s g_d g_{sd}/g_{ss})\Delta Y$, is at the ISR 3 mb ($\Delta Y \simeq 2$). Finally, the rise of the plateau in the one-particle inclusive spectrum is given, in our model, by $\Delta(d\sigma/dy) = g_s g_d g_{sd} \Delta Y$, and for the above values of the parameters we find a rise of 1.5 mb at the ISR. Although this latter value is somewhat smaller than the experimental one, the over-all picture is in reasonable agreement with the data. It follows that the internal inclusive dipole coupling of the Pomeron, g_{sd}, leads to a remarkable correlation among the following features of high-energy proton-proton scattering[8]:

(a) the smallness of the diffractive cross section,

(b) the small rise of the plateau,

(c) the small rise of the inelastic cross section.

Although the nondiffractive component is dominant at ISR and even higher energies, in the extreme asymptotic region ($Y \to \infty$) the diffractive component dominates the production mechanism. In fact the multiplicity distribution in this energy region can be determined from the asymptotic form of the quantities $\rho_q(Y)$ ($q = 1, 2, \ldots$) given by Eqs. (2) and (13).

We find

$$\langle n(n-1)\cdots(n-q+1)\rangle = \frac{g_s g_{ss}^{\,q-1} Y^q \{ g_s g_{ss} + [2/(q+1)] g_d g_{sd} Y \}}{g_s^{\,2} + g_d^{\,2} Y} \,. \tag{24}$$

From (24) follows

$$\lim_{Y\to\infty} \frac{\langle n^q \rangle}{\langle n \rangle^q} = \frac{2}{q+1} \left(\frac{g_{ss} g_d}{g_{sd} g_s} \right)^{q-1} \,. \tag{25}$$

Equation (25) shows that in the approximation of weak g_{sd} coupling the model satisfies Koba-Nielsen-Olesen (KNO) scaling in the limit $Y \to \infty$.

From the KNO moment equations

$$\int_0^\infty x^q P(x)\, dx = \frac{2}{q+1} \left(\frac{g_{ss} g_d}{g_{sd} g_s} \right)^{q-1} \,, \tag{26}$$

where $x = n/\langle n \rangle$ and $P(x) = \langle n \rangle \sigma_n/\sigma_{tot}$, we find

$$\begin{aligned} &\frac{\sigma_n}{\sigma_t} = \frac{2}{\langle n \rangle} \left(\frac{g_{sd} g_s}{g_{ss} g_d} \right)^2 \quad \text{for } n \leq \frac{g_{ss} g_d}{g_{sd} g_s} \langle n \rangle \,, \\ &\frac{\sigma_n}{\sigma_t} = 0 \qquad\qquad\quad \text{for } n \geq \frac{g_{ss} g_d}{g_{sd} g_s} \langle n \rangle \,. \end{aligned} \tag{27}$$

This is a typical form of a diffractive multiplicity distribution in which the average multiplicity $\langle n \rangle$ increases with energy because the cutoff $n_c = g_{ss} Y$ in the number of the produced particles increases logarithmically with energy, whereas the cross section $\sigma_n(Y)$ remains constant.

The discussion so far has been concerned with the implications of our model for the integrated quantities of the production process in the rapidity space such as the partial cross sections $\sigma_n(Y)$ and the total inelastic cross section $\sigma_{in}(Y)$. However, knowledge of the rapidity distribution of the inclusively produced particles allows determination of the rapidity distribution of the exclusively produced particles and therefore allows the detailed study of the features of our model.

Using the well-known formula[9]

$$\frac{d^n \sigma_{ex}}{dy_1 \cdots dy_n} = \sum_{l=0}^{\infty} \frac{(-1)^l}{l!} \int \frac{d^{n+l} \sigma_{in}}{dy_1 \cdots dy_n\, dy'_{n+1} \cdots dy'_{n+l}}\, dy'_{n+1} \cdots dy'_{n+l} \tag{28}$$

we find for the cases of one- and two-particle production in terms of the rapidities y_c, y_d in the lab system

$$\frac{d\sigma_1}{dy_c} = g_s^{\,2} g_{ss}\, e^{-g_{ss} Y} - \frac{g_s g_d g_{sd}}{g_{ss}} \left[2 e^{-g_{ss} Y} - e^{-g_{ss}(Y - y_c)} - e^{-g_{ss} y_c} \right] \,, \tag{29}$$

$$\frac{d^2\sigma_2}{dy_c\, dy_d} = g_s^{\,2} g_{ss}^{\,2}\, e^{-g_{ss} Y} - g_s g_d g_{sd} \left[2 e^{-g_{ss} Y} - e^{-g_{ss}(Y - y_c)} - e^{-g_{ss} y_d} \right] \tag{30}$$

for $y_c < y_d$.

Equation (29) shows that the exclusive one-particle distribution is enhanced near the walls as expected from the diffractive mechanism. This is due to the second term of Eq. (29), whereas the first term represents the constant background in the central region (pionization).

In general for the n-particle production we get

$$\frac{d^n\sigma_n}{dy_1 dy_2 \cdots dy_n} = g_s g_{ss}{}^{n-2}(g_s g_{ss}{}^2 - 2g_d g_{sd})\, e^{-g_{ss}Y} + g_s g_d g_{sd} g_{ss}{}^{n-2}\left[e^{-g_{ss}(Y-y_1)} + e^{-g_{ss}y_n}\right]. \tag{31}$$

The first term represents the multiperipheral component, whereas the other two terms represent the diffractive excitations of projectile and target, respectively.

One can examine in more detail the diffractive excitation mechanism by isolating the corresponding diffractive term in (31). In fact the missing-mass distribution for fixed n for the diffractive process is

$$\frac{d\sigma_n^{\,D}}{dM^2} = \frac{g_s g_d g_{sd}}{g_{ss}} \frac{(g_{ss}\ln M^2)^{n-1}}{(n-1)!} (M^2)^{-1-g_{ss}} . \tag{32}$$

Equation (32) represents[10] the single excitation of the proton by a fixed simple Pomeron with intercept 1.

The n particles produced in this diffractive dissociation are distributed according to a Poisson law arising from a multiperipheral mechanism. The meson trajectory exchanged along the multiperipheral chain is the one determined by the self-consistency relations (16).

More details on the calculation of (29), (30), and (31) are given in the Appendix.

III. PHENOMENOLOGICAL IMPLICATIONS

In this section we compare the results of our model with existing data on both inclusive and exclusive processes. The comparison is based on the values

$$g_s = 5.3\ \text{mb}^{1/2},\quad g_d = 1.4\ \text{mb}^{1/2},\quad g_{ss} = 1,\quad g_{sd} = 0.1$$

discussed in the previous section.

We first compare the correlation integrals of pp reactions with the latest cosmic-ray data at 10 TeV.[11] From (24) we calculate the quantities

$$g_1 = f_1 = \langle n\rangle,\quad g_2 = \langle n(n-1)\rangle,\quad g_3 = \langle n(n-1)(n-2)\rangle,$$
$$g_4 = \langle n(n-1)(n-2)(n-3)\rangle,\quad D = (\langle n^2\rangle - \langle n\rangle^2)^{1/2}, \tag{33}$$
$$\frac{\langle n\rangle}{D},\quad f_2 = g_2 - g_1^{\,2},\quad f_3 = g_3 - 3g_1 g_2 + 2g_1^{\,3},$$
$$f_4 = g_4 - 4g_1 g_3 + 12 g_1^{\,2} g_2 - 3g_2^{\,2} - 6g_1^{\,4} .$$

Table I shows the results of the calculations and the corresponding experimental values. We observe that there is a good agreement with data for the moments and f_2 but the correlations f_3 and f_4 deviate from the experimental values because of violent cancellations in their expressions.

The corresponding multiplicity distribution for the energy 10 TeV given by Eq. (18) is plotted in Fig. 2 along with the experimental data.[11] We observe that even at this extremely high energy the nondiffractive component is still dominant. It is also worth noting that the expected dip[12] has not yet appeared in this energy region either in experimental data or in our model.

TABLE I. Correlation integrals and some quantities of interest pertaining to multiplicity distributions at 10 TeV. ($g_{ss}=1$; $g_{sd}=0.1$.)

	Experiment	Theory
$\langle n\rangle$	7.1 ± 0.5	7.43
D	3.9 ± 0.4	4.60
$\langle n\rangle/D$	1.81 ± 0.2	1.62
g_2	59 ± 11	68.9
g_3	602 ± 185	661.4
g_4	$(7.2\pm3.1)\times10^3$	6.4×10^3
f_2	8.4 ± 4.1	13.7
f_3	57 ± 29	−54.24
f_4	173 ± 138	−97.7

$g_1=\langle n\rangle$, $g_2=\langle n(n-1)\rangle$, $g_3=\langle n(n-1)(n-2)\rangle$,
$g_4=\langle n(n-1)(n-2)(n-3)\rangle$,
$D=(\langle n^2\rangle-\langle n\rangle^2)^{1/2}$,
$f_1=g_1$, $f_2=g_2-g_1^{\,2}$, $f_3=g_3-3g_2g_1+2g_1^{\,3}$,
$f_4=g_4-4g_3g_1+12g_1^{\,2}g_2-3g_2^{\,2}-6g_1^{\,4}$.

Finally, a comparison is made of the exclusive two-particle distribution as given by formula (30) with experimental data for $\pi^+\pi^-$ production at 205 GeV/c.[13] In Fig. 3 the dependence of the exclusive differential cross section on the rapidity difference of the produced particles is plotted with the data. The expression obtained for this cross section after integrating formula (30) with respect to the sum of the secondary-particle rapidities, $y_+ = y_c + y_d$, is

$$\frac{d\sigma^{(2)}(y, Y)}{dy} = (g_s{}^2 g_{ss}{}^2 - 2g_s g_d g_{sd})\, e^{-g_{ss}Y}(Y-y) + \frac{2g_s g_d g_{sd}}{g_{ss}}\left(e^{-g_{ss}y} - e^{-g_{ss}Y}\right), \tag{34}$$

where $y = |y_c - y_d|$. One can easily verify that the integrated Eq. (34) agrees with Eq. (18) for $n=2$. We observe that both the size of the cross section and its rapid drop for increasing rapidity differences are borne out by our model.

IV. CONCLUSIONS

We have considered a model in which, together with a simple Pomeron, a dipole Pomeron is exchanged in the Regge-Mueller diagrams. Factorization was assumed by imposing the necessary

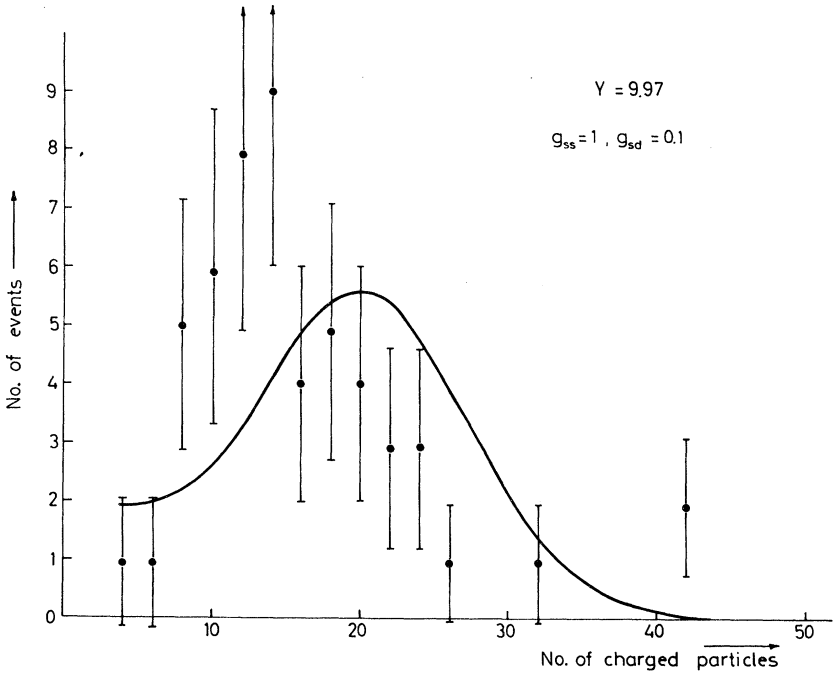

FIG. 2. The multiplicity distribution for $g_{ss}=1$, $g_{sd}=0.1$ plotted along with the data for charged particles at 10 TeV.

condition of a zero self-coupling of the dipole component.

We have shown that this model in the weak-coupling approximation is equivalent to a two-component model for the production mechanism, which leads to the following results:

(1) The dipole structure of the inclusive factorizable Pomeron generates in a self-consistent way the exclusive Pomeron with $\alpha_P(0)=1$. It also leads to an exclusive meson trajectory with $\alpha_M(0)=1-\frac{1}{2}g_{ss}$ ($g_{ss}\approx 1$).

(2) The total, the elastic, and the inelastic cross sections grow logarithmically with energy, in agreement with geometrical scaling and a logarithmic shrinking of the diffraction peak.

(3) The diffractive component of the inelastic cross sections in the ISR region and for $g_{sd}\approx 0.1$ is about 25% of the total inelastic cross section, in agreement with the data. In fact for $Y=7.5$ we find

$$\sigma_{\text{tot}}=42.8 \text{ mb}, \quad \sigma_{\text{in}}=37.7 \text{ mb},$$
$$\sigma_{\text{in}}^{\text{ND}}=28 \text{ mb}, \quad \sigma_{\text{in}}^{\text{D}}=9.7 \text{ mb}.$$

(4) The rise of the inelastic cross section and of the plateau is due to the diffractive component of the production mechanism, which in our model comes from the dipole component of the inclusive Pomeron.

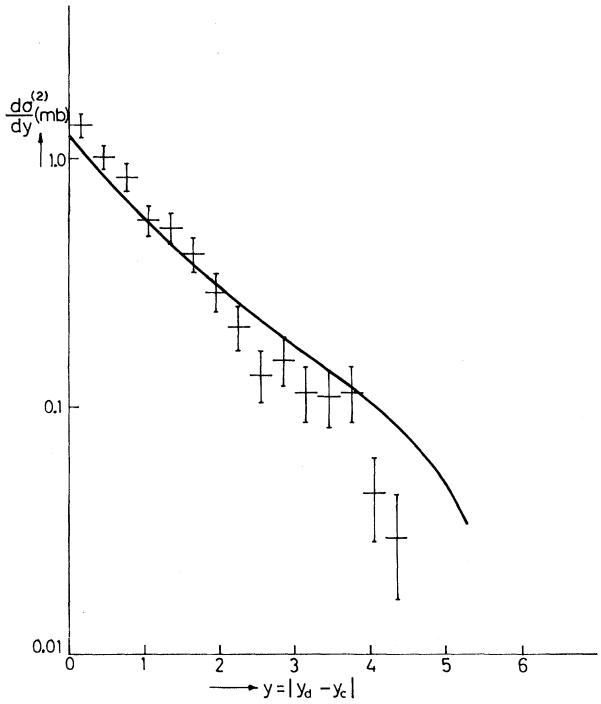

FIG. 3. The two-particle-production differential cross section versus the rapidity difference plotted with the $\pi^+\pi^-$ data at 205 GeV/c ($g_{ss}=1$, $g_{sd}=0.1$). The cross-section values given by Eq. (34) are multiplied by $\frac{2}{3}$ to account for the production of $\pi^+\pi^-$ pairs only.

(5) Asymptotically ($Y \to \infty$) the model is purely diffractive and satisfies KNO scaling.

(6) The multiplicity distribution predicted by the model is compatible with the existing data at ultrahigh energies.

(7) The exclusive production cross sections predicted in this model reveal the two-component structure (diffractive and nondiffractive) of the model. Moreover, the diffraction mechanism favored in this model is of the multiperipheral type.

(8) Comparison of the exclusive differential cross section for π^+, π^- production with Fermilab data at 205 GeV/c is made and the agreement is satisfactory.

ACKNOWLEDGMENT

We thank the members of the high energy experimental group at Argonne National Laboratory for permission to use the 205 GeV/c data on $d\sigma^{(2)}/dy$.

APPENDIX

Consider the Mueller diagram of Fig. 1 for l inclusively produced secondaries. In the weak g_{sd} limit there can be no dipole Pomeron coupled to a secondary-particle pair, since such an arrangement leads to an $O(g_{sd}^2)$ contribution to the differential exclusive cross sections.

The nondipole (ND) contribution to $d\sigma_1/dy_c$ is given [see Eq. (28)] by

$$\frac{d\sigma_1^{\mathrm{ND}}}{dy_c} = \sum_{l=1}^{\infty} (-1)^{l-1} g_s^{\,2} g_{ss}^{\,l} \sum_{i=1}^{l} \int_{y_c}^{Y} dy_l\, P(Y-y_l) \cdots \int_{y_c}^{y_{i+2}} dy_{i+1} P(y_{i+2}-y_{i+1})\, P(y_{i+1}-y_c) \times \int_0^{y_c} dy_{i-1} \cdots \int_0^{y_2} dy_1 P(y_2-y_1)\, P(y_1)\,, \tag{A1}$$

where $P(y) = e^y$.

The same equation is used to obtain $d\sigma_1^{\mathrm{D}}/dy_c$, except that the factor $P(Y-y_l)$ [or $P(y_1)$] is replaced by $D(Y-y_l)$ [or $D(y_1) = y_1 e^{y_1}$], and $g_s^{\,2} g_{ss}^{\,l}$ by $g_s g_d g_{sd} g_{ss}^{\,l-1}$. Taking the Laplace transform of the convolution integrals in (A1) one obtains $d\sigma_1/dy_c = d\sigma_1^{\mathrm{ND}}/dy_c + d\sigma_1^{\mathrm{D}}/dy_c$ as given in the text [Eq. (29)].

The Mueller diagrams which build up the $d^l\sigma_l/dy_1, \ldots, dy_l$ for $l \geq 2$ are similarly divided into two classes, diffractive and nondiffractive. The same procedure is then followed to prove Eq. (30) or in general (31).

[1] G. F. Chew and A. Pignotti, Phys. Rev. 176, 2112 (1968).
[2] H. D. I. Abarbanel and J. B. Bronzan, Phys. Lett. 48B, 345 (1974).
[3] N. G. Antoniou, C. B. Kouris, and G. M. Papaioannou, Phys. Lett. 52B, 207 (1974).
[4] W. A. Bardeen and R. D. Peccei, Phys. Lett. 45B, 353 (1973).
[5] V. Barger, in *Proceedings of the XVII International Conference on High Energy Physics, London, 1974*, edited by J. R. Smith (Rutherford Laboratory, Chilton, Didcot, Berkshire, England, 1974), p. I-193.
[6] N. G. Antoniou, C. B. Kouris, E. K. Manesis, and G. M. Papaioannou, Phys. Lett. 55B, 77 (1975).
[7] The value $g_{ss} \approx 1$ is consistent with the height of the plateau $d\sigma/dy = 29$ mb observed at the CERN ISR, whereas the interpretation of the third term in (14) as the interference of the Pomeron with the meson would lead to $\alpha_M(0) = 1 - g_{ss}$ and a normal trajectory would give $g_{ss} = 0.5$, corresponding to a considerably lower value of the plateau ($d\sigma/dy \approx 19$ mb).
[8] E. L. Berger, CERN Report No. TH. 1737, 1973 (unpublished).
[9] Z. Koba, H. B. Nielsen, and P. Olesen, Nucl. Phys. B43, 125 (1972).
[10] H. Harari, Weizmann Institute Report No. WIS 73/32 Ph (unpublished).
[11] B. S. Chaudhary and P. K. Malhotra, Nucl. Phys. B86, 360 (1975).
[12] K. Fiałkowski and H. I. Miettinen, Phys. Lett. 43B, 61 (1973).
[13] H. Yuta, private communication.